

Farnesyltransferase inhibitors induce dramatic morphological changes of KNRK cells that are blocked by microtubule interfering agents

NOBUTAKA SUZUKI, KEITH DEL VILLAR, AND FUYUHIKO TAMANOI*

Department of Microbiology and Molecular Genetics, Jonsson Comprehensive Cancer Center, University of California, Los Angeles, 405 Hilgard Avenue, Los Angeles, CA 90095-1489

Communicated by John A. Glomset, University of Washington, Seattle, WA, June 26, 1998 (received for review March 27, 1998)

ABSTRACT Farnesyltransferase inhibitors (FTIs) exhibit the remarkable ability to inhibit transformed phenotypes of a variety of human cancer cell lines and to block the growth of cancer cells in a number of animal model systems. In this paper, we report that the addition of FTI to *v-K-ras*-transformed NRK cells (KNRK) results in dramatic morphological changes. Within 24 h after the addition of FTI, the round morphology of KNRK cells was changed to an elongated (flattened and spread out) morphology resembling those of untransformed NRK cells. No morphological effects were seen when similar concentrations of FTI were added to NRK cells. Phalloidin staining showed that FTI treatment did not restore the disrupted actin cytoskeleton in KNRK cells. In contrast, FTI addition resulted in the appearance of extensive microtubule networks in KNRK cells. The addition of a low concentration (1.2 nM) of vincristine or vinblastine, agents that interfere with microtubule dynamics, blocked the FTI-induced morphological changes in KNRK cells. In contrast, cytochalasin B, which interferes with actin polymerization, did not block the morphological changes. The FTI-induced morphological changes were associated with a decrease in the percentage of cells in S-phase, and the addition of 1.2 nM vincristine did not have additional effects on cell cycle progression. A higher concentration (12 nM) of vincristine caused synergistic effect with FTI to enrich dramatically KNRK cells in G₂/M phase. These results suggest that FTI affects cell morphology and that microtubule dynamics are involved in these processes.

Farnesyltransferase inhibitors (FTIs) have emerged as promising anti-cancer drugs (1, 2). These compounds inhibit protein farnesyltransferase, an enzyme that catalyzes farnesylation of proteins ending with the CAAX motif (C is cysteine, A is an aliphatic amino acid, and X is the C-terminal amino acid) (1–3). FTIs inhibit anchorage-independent growth of a variety of transformed cells (4, 5). A survey of cancer cell lines has shown that >70% of cells are sensitive to FTI (6). In addition, FTIs have been shown to inhibit the growth of tumors in a number of animal model studies (7–10). In one case, regression of mammary tumors in transgenic mice expressing activated *H-ras* was observed (10). These promising drugs currently are being assessed in clinical trials (11).

Remarkably, FTIs show little effects on untransformed cells (2). Furthermore, FTIs did not exhibit any significant toxicity in animal studies (2). This specific effect of FTIs on transformed cells raises the possibility that farnesylated proteins play critical roles in maintaining transformed phenotypes. Although farnesylation of Ras initially was thought to be

responsible for the effects of FTIs, a number of recent observations raise the possibility that farnesylation of proteins other than Ras is important for the effects of FTIs (2, 12). First, it has been shown that FTIs are incapable of inhibiting the modification of K-ras and N-ras. Instead of accumulating as unmodified proteins, they are modified by a geranylgeranyl group in the presence of FTIs (13, 14). Second, FTIs inhibit transformed phenotypes of cancer cell lines irrespective of whether they contain mutated *ras* (6). An increasing number of farnesylated proteins, in addition to Ras, have been identified (12). These include members of the Rho-family of G proteins such as RhoB (15, 16) and RhoE (17), another G protein Rheb (18) as well as inositol-1,4,5-triphosphate 5-phosphatase (19, 20) and cyclic nucleotide phosphodiesterase (21, 22).

Because the phenotypes induced by FTIs may provide hints about farnesylated proteins critical for maintaining transformed phenotypes, we have initiated a study to characterize effects of FTIs on the physiology of transformed cells. Although a variety of biological effects of FTIs including inhibition of soft agar growth, morphological reversions (23, 24), cell cycle progression (25, 26), and induction of apoptosis (apoptosis of tissue culture cells is seen only when cells are denied attachment to substratum) (25, 27) has been reported, a clear picture of the effect of FTIs on transformed cells has not emerged. In this work, we focused on morphological changes induced by FTIs with the hope to investigate the effects of FTIs on cellular cytoskeletons. To carry out a detailed investigation of the FTI-induced morphological changes, we took advantage of transformed cells that exhibit a round morphology. Changes of the morphology of such cells would be dramatic and should enable us to investigate associated cytoskeletal changes. After examining a number of transformed cell lines, we realized that *v-K-ras*-transformed NRK cells (KNRK) provide a suitable system. In this paper, we present evidence that FTIs cause dramatic morphological changes of KNRK cells and that microtubules play an important role in these changes.

MATERIALS AND METHODS

Materials. Two types of FTIs were used in this study. SCH56582 is a derivative of SCH44342, a tricyclic inhibitor of protein farnesyltransferase (24). They were provided by W. Robert Bishop (Schering-Plough). B1088 is a derivative of B1086, a peptidomimetic inhibitor of farnesyltransferase derived from a tetrapeptide CVFM (8). B1088 was provided by Ana Maria Garcia (Eisai Research Institute). Microtubule

The publication costs of this article were defrayed in part by page charge payment. This article must therefore be hereby marked "advertisement" in accordance with 18 U.S.C. §1734 solely to indicate this fact.

© 1998 by The National Academy of Sciences 0027-8424/98/9510499-6\$2.00/0
PNAS is available online at www.pnas.org.

Abbreviations: FTI, farnesyltransferase inhibitor; NRK, normal rat kidney; KNRK, *v-K-ras* transformed NRK; VCR, vincristine; CYB, cytochalasin B.

*To whom reprint requests should be addressed. e-mail: fuyut@microbio.ucla.edu.

inhibitors vincristine and vinblastine, as well as cytochalasin B, were obtained from Sigma.

Cells. KNRK cells (CRL-1569) as well as NRK cells (CRL-1570) were obtained from American Type Culture Collection. KNRK cells are NRK cells transformed with *v-K-ras* (28). Spon 5 and Spon 8 cells are tumorigenic, metastatic mouse lung cancer cells (29) and were provided by Ming You (Ohio State University). Cells were grown in DMEM containing 10% fetal calf serum.

Immunofluorescence and Western Blotting. To visualize polymerized actin, cells were fixed in 4% paraformaldehyde for 10 min, permeabilized with 0.5% Triton X-100 for 10 min, and incubated with 1 $\mu\text{g}/\text{ml}$ fluorescein isothiocyanate-labeled phalloidin (Sigma) for 1 h. Antibody against actin (Sigma) also was used for indirect immunofluorescence. For microtubule localization, cells were fixed with -80°C methanol/acetone (1:1) for 10 min and permeabilized with 0.5% Triton X-100 for 10 min. They were incubated with a 1:2,000 dilution of the monoclonal α -tubulin antibody B-5-1-2 (Sigma) for 1 h at 37°C . This was followed by a 45-min incubation with a 1:1,000 dilution of fluorescein isothiocyanate-conjugated goat anti-mouse IgG (Sigma). Cells were viewed on a Nikon microscope and photographed with Kodax T-MAX 400 film. Western blotting was carried out according to the method described in ref. 13. mAb TM311 against high molecular weight isoforms of tropomyosin was obtained from Sigma.

Flow Cytometry. Cells treated with or without FTI were analyzed by propidium iodide staining and flow cytometry with a FACScan flow cytometer (Becton Dickinson Immunocytometry Systems) as described (30). Histograms were analyzed for cell cycle compartment by using CELLQUEST software (Becton Dickinson Immunocytometry Systems). Ten thousand events were collected to maximize the statistical validity of the compartmental analysis. Percentage of live cells was determined by staining cells with 7-aminoactinomycin D (31). This procedure also determines the percentage of apoptotic cells and dead cells.

RESULTS

FTI Causes Morphological Changes of *v-K-ras*-Transformed NRK Cells. To identify a transformed cell line that exhibits dramatic morphological changes in response to the addition of FTIs, we examined a number of established cancer cell lines. From this survey, we found that FTIs cause distinct morphological changes of *v-K-ras*-transformed NRK cells (KNRK). In most of the studies reported in this paper, we used SCH56582, a tricyclic compound that acts as a competitive inhibitor of farnesyltransferase with respect to its substrate protein (24). This compound is effective in inhibiting anchorage-independent growth of transformed cells (13, 24). We also have confirmed that the growth of KNRK cells on soft agar is inhibited by SCH56582 (data not shown). The effects of SCH56582 on the morphology of KNRK cells are shown in Fig. 1. KNRK cells have a round morphology (Fig. 1A) whereas untransformed NRK cells have an elongated (flattened and stretched) morphology (Fig. 1C). After the addition of SCH56582, the round KNRK cells became elongated, and extensions were seen (Fig. 1B). In contrast, no changes were seen with the morphology of untransformed NRK cells by the addition of SCH56582 (compare Fig. 1C and D). The FTI-induced morphological changes of KNRK cells depend on SCH56582 concentration. Approximately 50% of cells exhibited elongated morphology after the treatment with 10 μM SCH56582, and the percentage of cells with this altered morphology reached $\approx 75\%$ with 20 μM SCH56582 treatment (Fig. 2A). In contrast, we did not see any effects of these concentrations of SCH56582 on NRK cells at least up to 48 h. Concentrations >60 μM interfered with the growth of both KNRK and NRK cells. The time course of the morphological

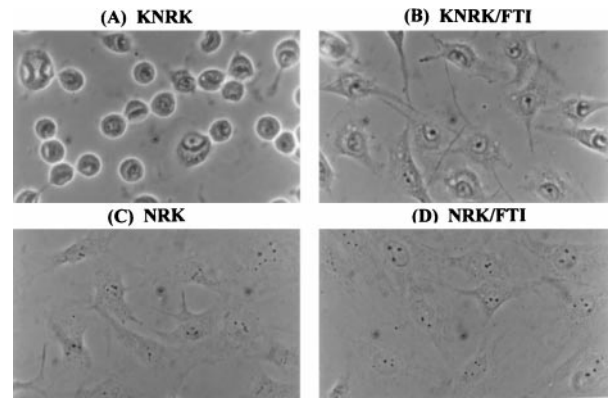


FIG. 1. Effects of FTI (SCH56582) on the morphology of NRK and KNRK cells. NRK and KNRK cells were plated at the density of 5×10^4 cells/well in a 4-well chamber slide (LAB-TEK) and, after 24 h, treated with DMSO (A and C) or with 20 μM SCH56582 (B and D). The phase-contrast images were captured at $\times 400$ magnification 24 h after the FTI addition. (A) KNRK. (B) KNRK treated with 20 μM SCH56582. (C) NRK. (D) NRK treated with 20 μM SCH56582. At least three separate experiments were carried out with results similar to those shown here.

changes (Fig. 2B) shows that the changes occur by 24 h after the addition of SCH56582, and $>60\%$ of cells change their morphology by 36 h after the SCH56582 addition. The effects of SCH56582 on the morphology of KNRK cells appear to be reversible because round cells reappeared 3 days after the removal of SCH56582 (data not shown).

Similar morphological changes were observed with a different type of inhibitor, B1088 (8), a peptidomimetic of a CAAX peptide, CVFM; 60 μM B1088 caused $\approx 70\%$ of cells to change their morphology (data not shown). SCH56582 also induced morphological changes in tumorigenic, metastatic mouse lung epithelial cells, Spon5 and Spon8 (29); $>70\%$ of these round cells became elongated in response to 24 h of treatment with 20 μM SCH56582 (data not shown).

FTI Does Not Restore Actin Cytoskeleton Disrupted in KNRK Cells. To investigate further the mechanisms involved in the morphological changes caused by FTI, we examined the actin cytoskeleton by indirect immunofluorescence of cells (Fig. 3). NRK cells stained with phalloidin showed extensive actin cytoskeleton networks as seen by their typical fiber-like appearance (Fig. 3A). In contrast, fiber-like staining was not observed with KNRK cells, and the phalloidin staining was observed more at the cell periphery (Fig. 3B). Phalloidin staining of KNRK cells after the treatment with SCH56582 was similar to that seen with the untreated KNRK cells (Fig. 3C); although cell morphology was changed, the staining still was detected at the periphery of cells. Staining with anti-actin antibody also showed that SCH56582 failed to restore the disrupted actin cytoskeleton in KNRK cells (data not shown). SCH56582 also failed to induce focal adhesion plaques; typical punctate staining by anti-vinculin antibody was not observed (data not shown). We also examined effects of FTI on tropomyosin, which is involved in the regulation of actin cytoskeleton. It has been reported that NRK cells express three isoforms of high molecular weight tropomyosin, TM-1, TM-2, and TM-3, and that TM-2 and TM-3 are missing in KNRK cells (32). In agreement with this report, we detected TM-1 but not TM-2 or TM-3 in heat-treated extracts of KNRK cells, whereas all three tropomyosin isoforms were detected in heat-treated extracts of NRK cells. Treatment of KNRK cells with 20 μM SCH56582 did not influence this tropomyosin expression pattern in KNRK cells, and neither TM-2 nor TM-3 was detected (data not shown). Taken together, these results suggest that SCH56582 does not affect the actin cytoskeleton.

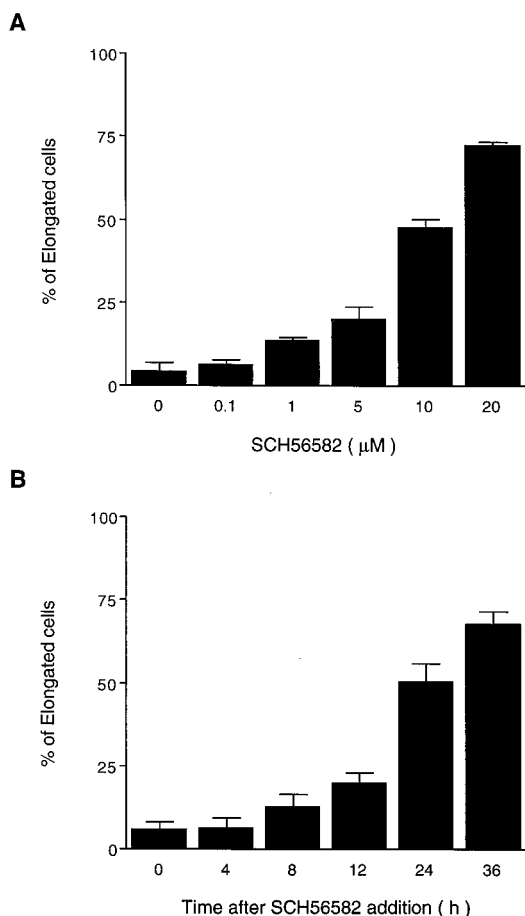


FIG. 2. Dose- and time-dependent effects of FTI on the morphology of KNRK cells. (A) KNRK cells were plated as described in the legend to Fig. 1. Cells were treated with 0.1, 1, 5, 10, or 20 μM SCH56582. The number of elongated cells was determined 24 h after the treatment by counting the number of elongated cells (flattened cells with extensions) and round cells in 100–200 randomly selected cells. (B) KNRK cells were treated with 10 μM SCH56582. The number of elongated cells was determined 4, 8, 12, 24, and 36 h after the treatment. SD are shown by vertical bars.

FTI Causes Significant Effects on Microtubule Networks. In contrast to the lack of effects on the actin cytoskeleton, we observed significant effects of SCH56582 on microtubule networks. Fig. 4 shows indirect immunofluorescence of cells stained with anti- α -tubulin antibody. Typical extensive microtubule fibers were found in NRK cells (Fig. 4A). In contrast, microtubule networks were much less extensive in KNRK cells; the anti-tubulin staining in KNRK cells was more predominant at the cell periphery (Fig. 4B). A region of intense staining also is seen in the cytoplasm, presumably representing that of the microtubule organization center. The addition of SCH56582 led to the expansion of the microtubule networks, and extensive fibers now are observed in the FTI-treated KNRK cells (Fig. 4C). Western analyses showed that the level of α - and β -tubulins in KNRK cells was not significantly different from that in NRK cells and that these levels were not affected by the addition of SCH56582 (data not shown). Thus, it appears that SCH56582 causes a significant change of the microtubule networks rather than affecting the synthesis of tubulins.

Microtubule Interfering Agents Block the FTI-Induced Morphological Changes of KNRK Cells. The appearance of extensive networks of microtubules in the FTI-treated KNRK cells raises the possibility that microtubule extension is important for the FTI-induced morphological changes. Alternatively, FTI induces morphological changes by a mechanism

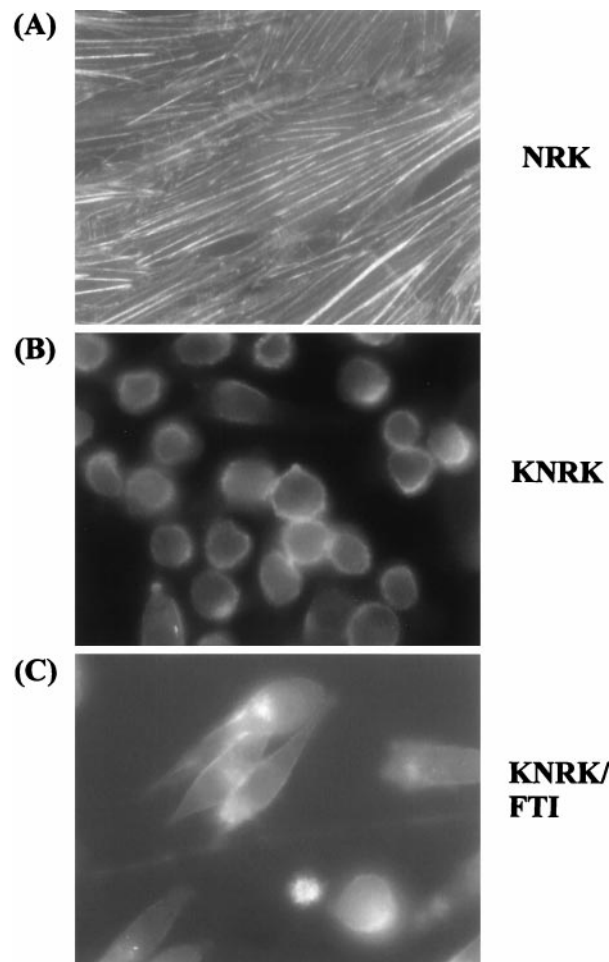


FIG. 3. Immunofluorescence microscopy of actin stress fibers. NRK and KNRK cells were seeded on 4-well chamber slides and treated the following day with DMSO or with 20 μM SCH56582. After 24 h, cells were washed and fixed in 4% paraformaldehyde and stained with fluorescein isothiocyanate-labeled phalloidin as described in *Materials and Methods*. (A) NRK. (B) KNRK. (C) KNRK treated with 20 μM SCH56582. The stained images were captured at $\times 400$ magnification. At least three experiments were carried out with results similar to those shown here.

independent of microtubules and that microtubule extension occurs as a consequence of the morphological change. To investigate these points, we used vincristine or vinblastine, compounds that interfere with the dynamic process of microtubule assembly. Fig. 5 shows the effects of vincristine on FTI-induced morphological changes. As can be seen, vincristine effectively blocked the FTI-induced morphological changes (Fig. 5, compare D to B and A). The block of FTI-induced morphological changes of KNRK cells can be obtained with vincristine concentrations as low as 1.2 nM. At this low concentration, vincristine alone does not exhibit any significant effects on the morphology of KNRK cells (data not shown) and does not affect cell cycle progression (see below; Table 1). A similar block of the FTI-induced morphological changes was obtained with vinblastine or with colchicine (data not shown). In marked contrast to the results obtained with microtubule-interfering agents, the addition of 2.1 μM cytochalasin B, a compound that interferes with actin polymerization, did not affect the FTI-induced morphological changes of KNRK cells (Fig. 5C). Although it is not obvious in Fig. 5, we did observe a small percentage of binucleated cells among KNRK cells treated with FTI plus cytochalasin B. Cytochalasin B alone does not exhibit any significant effects on morphology and cell cycle progression of KNRK cells (data not shown).

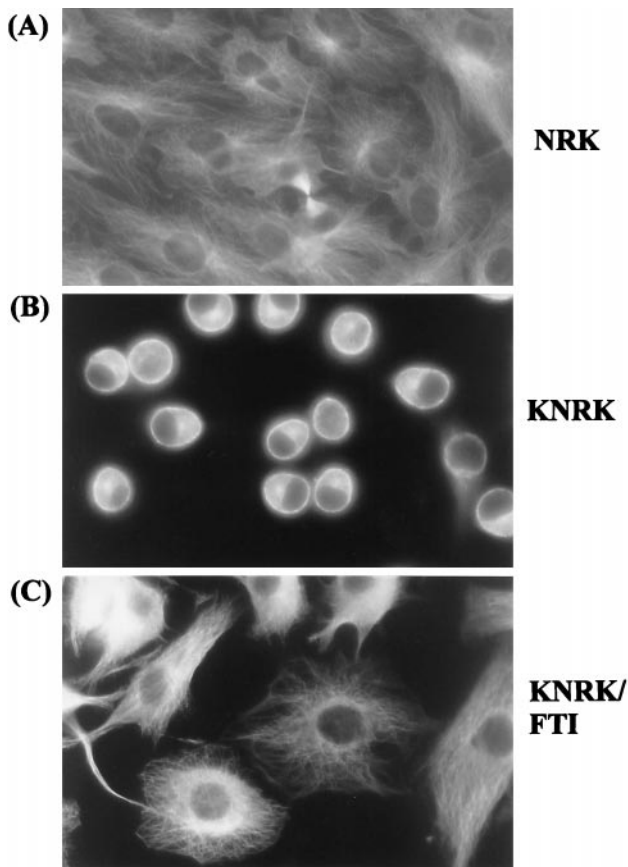


FIG. 4. Immunofluorescence microscopy of microtubules. NRK and KNRK cells were seeded on 4-well chamber slides and treated the following day with DMSO or with 20 μM SCH56582. After 24 h, cells were fixed with methanol/acetone (1:1) (-80°C) and were stained with α -tubulin described in *Materials and Methods*. (A) NRK. (B) KNRK. (C) KNRK treated with 20 μM SCH56582. The stained images were captured at $\times 400$ magnification. At least three experiments were carried out with results similar to those shown here.

Taken together, these results support the idea that microtubule dynamics are critical for the action of FTI.

The FTI-Induced Morphological Changes Are Associated with the Decrease of S-Phase Cells. FACS analyses of KNRK cells treated with FTI revealed that these cells have a significantly lower percentage of S-phase cells compared with untreated cells. As shown in Table 1, the percentage of KNRK cells in S-phase was 43.4% before the treatment. This was decreased to 21.2% after the treatment with SCH56582. This decrease in S-phase cells was accompanied by increases in the percentage of cells in G₁-phase (49.2–66.7%) as well as in G₂/M-phase (7.4–12.2%). In contrast to its effect on KNRK cells, SCH56582 had little effects on the cell cycle distribution of NRK cells. The percentage of S-phase cells and G₁-phase cells remained similar between the untreated and treated NRK cells (14.2 vs. 10.9% for S-phase cells; 60 vs. 60.8% for G₁-phase cells). Thus, SCH56582 causes KNRK cells to alter cell cycle progression so that the cell cycle distribution is more similar to that of NRK cells. The decrease of S-phase cells in KNRK parallels the effect of FTI on the growth rate of KNRK cells. KNRK cells grow with a doubling time of 21 h, whereas the doubling time of NRK cells is 55 h. The addition of SCH56582 to KNRK cells resulted in the reduction of the growth rate so that the doubling time is 46 h, which is comparable to that of NRK cells. On the other hand, SCH56582 did not have significant effects on the growth rate of NRK cells.

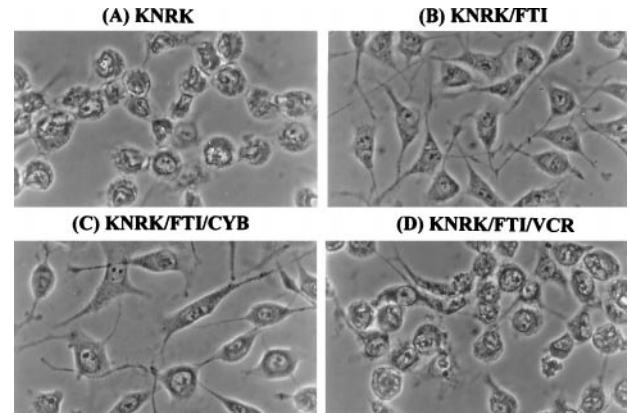


FIG. 5. Effects of vincristine (VCR) and cytochalasin B (CYB) on FTI-induced morphological changes of KNRK cells. KNRK cells were pretreated with DMSO (A and B) or with 2.1 μM CYB (C) or with 1.2 nM VCR (D). After 24 h, cells were treated with 20 μM SCH56582 for 24 h. (A) KNRK. (B) KNRK treated with SCH56582. (C) KNRK treated with SCH56582 and CYB. (D) KNRK treated with SCH56582 and VCR. At least three experiments were carried out with results similar to those shown here.

We also examined whether vincristine used to block the above FTI-induced morphological changes affected cell cycle distribution of KNRK cells. As can be seen in Table 1, vincristine at a 1.2-nM concentration did not significantly affect the cell cycle distribution of FTI-treated KNRK cells (compare KNRK, FTI, and FTI + VCR). In addition, 1.2 nM vincristine alone did not significantly affect cell cycle distribution of KNRK cells (compare KNRK, None, and VCR). Therefore, vincristine at 1.2 nM blocks the FTI-induced morphological changes of KNRK cells without affecting their cell cycle distribution.

FTI Together with a High Concentration of Vincristine Causes Enrichment of G₂/M-Phase Cells. Although vincristine at 1.2 nM concentration does not affect cell cycle distribution of FTI-treated KNRK cells, higher concentrations of vincristine cause enrichment of cells in the G₂/M phase. This G₂/M enrichment is due to the interference of vincristine on microtubule dynamics that are critical for chromosome segregation during mitosis. As shown in Fig. 6B, 12 nM vincristine caused enrichment of cells in the G₂/M phase (the percentage of G₂/M phase cells was 19.4% compared with 7.7% for the control). When FTI was added together with 12 nM vincristine, a dramatic enrichment of G₂/M phase cells was seen (Fig. 6C) and the percentage of G₂/M phase cells reached 55.5%. Thus, FTI shows synergy with vincristine to enrich cells in the G₂/M phase. Most of these cells contained disordered abnormal spindle apparatus. We also noticed that the majority of KNRK cells was detached after the treatment with vincristine

Table 1. Cell cycle characteristics

Cell	Treatment	% of cells in phase:		
		G ₁	S	G ₂ /M
KNRK	None	49.2	43.4	7.4
	FTI	66.7	21.2	12.2
NRK	None	60.0	14.2	25.7
	FTI	60.8	10.9	28.3
KNRK	VCR	55.2	40.5	4.3
	FTI + VCR	67.2	18.7	14.1

Cells were seeded at 5×10^5 cells/10-cm dish and treated the following day with 20 μM SCH56582 or 1.2 nM vincristine (VCR) or 20 μM SCH56582 plus 1.2 nM VCR. After 24 h of treatment, cells were harvested and cell cycle distribution was determined as described in *Materials and Methods*. Ten thousand cells were examined in each experiment.

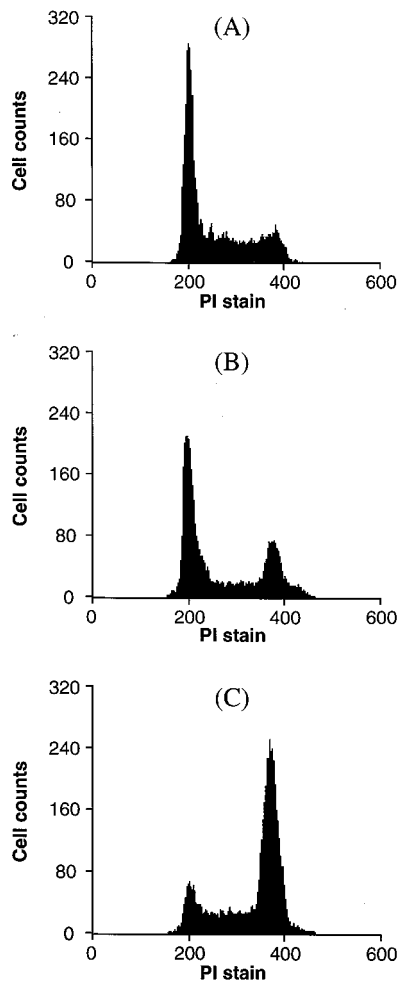


FIG. 6. Effect of FTI and 12 nM vincristine on cell cycle progression. KNRK cells were seeded at 5×10^5 cells/10-cm dish and treated the following day with DMSO (A) or 12 nM vincristine (B) or 20 μ M SCH56582 plus 12 nM vincristine (C). After 24 h, cells were harvested and cell cycle distribution was determined by using flow cytometry as described in *Materials and Methods*. At least 10,000 cells were examined in each assay. (A) KNRK. (B) KNRK treated with 12 nM VCR. (C) KNRK treated with 12 nM VCR and 20 μ M SCH56582.

and FTI. The percentage of live cells, $\approx 90\%$ as assessed by the staining with 7-aminoactinomycin D, was unaffected by the treatment.

DISCUSSION

An implication of the present study is that microtubule dynamics play critical roles in the effects of FTI on KNRK cells. Extensive microtubule networks are seen readily with untransformed NRK cells, but such networks are less extensive in KNRK cells. The addition of FTI to KNRK cells results in dramatic morphological changes and reappearance of extensive microtubule networks (Fig. 4). This suggests that FTI induces the extension of microtubules in the cytoplasm. We speculated that, if this were the case, the addition of microtubule interfering agents such as vincristine or vinblastine would block FTI-induced morphological changes of KNRK cells. This was shown to be the case with SCH56582- or B1088-induced morphological changes. In addition, FTI-induced changes of Spon8 cells were sensitive to vincristine. Microtubules are under dynamic equilibrium between polymers and tubulin monomers/dimers. Binding of vincristine to tubulin monomers and dimers upsets this equilibrium (33) and blocks microtubule extension. We noted that the concentration

of vincristine needed to block the FTI-induced morphological changes could be as low as 1.2 nM. At this concentration, no significant effects on cell cycle distribution were observed. FTI may be involved in a step in the restoration of microtubule networks that requires a particularly high concentration of tubulin monomers and dimers, and this step is highly sensitive to the addition of vincristine.

The effect of FTI on microtubule dynamics also may explain our observation that the addition of both FTI and vincristine causes enrichment of G₂/M phase cells. This synergistic effect of vincristine and FTI was seen at a concentration of vincristine 10 times higher than that required to block the FTI-induced morphological changes. During mitosis, microtubules completely reorganize to carry out chromosome segregation. The reorganization of microtubules requires dynamic and highly regulated polymerization and depolymerization events. Interference of this dynamic process by the binding of vincristine to tubulin monomers and dimers results in the enrichment of G₂/M phase cells. FTI might interfere further with this dynamic by incorrectly providing a signal for microtubule extension when it is necessary to depolymerize microtubules. A similar synergistic effect of FTI and a microtubule drug was reported by Moasser *et al.* (34) who showed that FTI significantly enhanced taxol-induced arrest of MCF-7 breast cancer cells at the G₂/M phase.

If one of the critical functions of FTI is to affect microtubule dynamics, it is possible that farnesylated proteins are involved in the modulation of microtubules. It may be the case that farnesylated proteins associate with microtubules and directly affect their regulation. In this regard, it is interesting to note that cyclic nucleotide phosphodiesterase (CNPase) (21, 22) has been reported to be associated with microtubules (35). There are two isoforms of CNPase, CNP1 (46 kDa) and CNP2 (48 kDa), and both contain the C-terminal CysThrIleIle sequence. Characterization of these proteins showed that they can be modified by either a farnesyl or a geranylgeranyl group (36). Additional investigation is needed to examine the prenylation status of CNP1 and CNP2 proteins in KNRK cells and to see whether FTI blocks farnesylation of these proteins.

An alternative possibility for how FTI can modulate microtubule dynamics is that FTI affects a signaling pathway that is involved in the regulation of proteins affecting microtubules. Posttranslational modifications of these proteins such as microtubule associated proteins (MAPs) are believed to be critical for the stability of microtubules. Possibly, farnesylated proteins activate such protein kinases. An example of a class of protein kinases modulating microtubule functions is extracellular signal-regulated kinases (ERKs) also known as mitogen-activated protein kinases (MAPKs). Constitutive activation of ERKs by the expression of a mutant form of MAPK kinase is associated with morphological rounding and a loss of cytoskeletal organization, whereas the inhibition of ERK activity leads to cytoskeletal organization and morphological flattening of transformed NIH 3T3 cells (37, 38). Expression of a mutant form of ERK2 also affects cytoskeletal organization (39). Association of ERKs with microtubules places these kinases in close proximity to microtubule-associated proteins (40). Activity of protein kinases similar to ERKs might be affected by FTI. We do not believe that FTI affects ERKs because FTI does not alter the expression and activation of ERK1 and ERK2 in KNRK cells (unpublished observation). Furthermore, FTI does not affect modification of v-K-ras protein, which functions upstream of ERKs. The addition of FTI did not result in the appearance of unmodified v-K-ras protein on a SDS polyacrylamide gel, whereas such unmodified proteins were detected with extracts from mevlinin-treated cells (unpublished observation). Investigation of signaling pathways affected by FTI should provide further insights into the action of FTI.

In conclusion, we have obtained evidence that FTI affects microtubule dynamics. Additional work to examine whether FTI causes any biochemical changes in microtubules as well as in proteins associating with microtubules may be informative. This line of investigation may provide hints about the identity of farnesylated proteins affected by FTI, and this may lead to our understanding of the roles of farnesylated proteins in maintaining transformed phenotypes.

We thank Dr. W. Robert Bishop for providing SCH56582. We are grateful to Dr. Peter Edwards for critical reading of the manuscript and to Dr. A. K. Rajasekaran for valuable suggestions on indirect immunofluorescence. We thank Ingrid Schmid and Nathan Regimbal in the UCLA Flow Cytometry Core Laboratory for assistance on flow cytometry analysis. We thank Dr. Fumio Matsumura for advice on tropomyosin studies. This work is supported by National Institutes of Health Grant CA41996.

1. Sattler, I. & Tamanoi, F. (1996) in *Regulation of the RAS Signaling Network*, eds. Maruta, H. and Burgess, A. W., RG Landes, Austin, pp 95–137.
2. Gibbs, J. B. & Oliff, A. (1997) *Annu. Rev. Pharmacol. Toxicol.* **37**, 143–166.
3. Zhang, F. L. & Casey, P. J. (1996) *Annu. Rev. Biochem.* **65**, 241–269.
4. James, G. L., Goldstein, J. L., Brown, M. S., Rawson, T. E., Somers, T. C., McDowell, R. S., Crowley, C. W., Lucas, B. K., Levinson, A. D. & Marsters, J. C., Jr. (1993) *Science* **260**, 1937–1942.
5. Kohl, N. E., Mosser, S. D., deSolms, S. J., Giuliani, E. A., Pompliano, D. L., Graham, S. L., Smith, R. L., Scolnick, E. M., Oliff, A. & Gibbs, J. B. (1993) *Science* **260**, 1934–1937.
6. Sepp-Lorenzino, L., Ma, Z., Rands, E., Kohl, N. E., Gibbs, J. B., Oliff, A. & Rosen, N. (1995) *Cancer Res.* **55**, 5302–5309.
7. Kohl, N. E., Wilson, F. R., Mosser, S. D., Giuliani, E., deSolms, S. J., Conner, M. W., Anthony, N. J., Holtz, W. J., Gomez, R. P., Lee, T. J., *et al.* (1994) *Proc. Natl. Acad. Sci. USA* **91**, 9141–9145.
8. Nagasu, T., Yoshimatsu, K., Rowell, C., Lewis, M. D. & Garcia, A. M. (1995) *Cancer Res.* **55**, 5310–5314.
9. Sun, J., Qian, Y., Hamilton, A. D. & Sebti, S. M. (1995) *Cancer Res.* **55**, 4243–4247.
10. Kohl, N. E., Omer, C. A., Conner, M. W., Anthony, N. J., Davide, J. P., deSolms, S. J., Giuliani, E. A., Gomez, R. P., Graham, S. L., Hamilton, K., *et al.* (1995) *Nat. Med.* **1**, 792–797.
11. Barinaga, M. (1997) *Science* **278**, 1036–1039.
12. Cox, A. D. & Der, C. J. (1997) *Biochim. Biophys. Acta* **1333**, F51–F71.
13. Whyte, D. B., Kirschmeier, P., Hockenberry, T. N., Nunez-Oliva, I., James, L., Catino, J. J., Bishop, W. R. & Pai, J. K. (1997) *J. Biol. Chem.* **272**, 14459–14464.
14. Rowell, C. A., Kowalczyk, J. J., Lewis, M. D. & Garcia, A. M. (1997) *J. Biol. Chem.* **272**, 14093–14097.
15. Lebowitz, P. F., Davide, J. P. & Prendergast, G. C. (1995) *Mol. Cell. Biol.* **15**, 6613–6622.
16. Lebowitz, P. F., Casey, P. J., Prendergast, G. C. & Thissen, J. A. (1997) *J. Biol. Chem.* **272**, 15591–15594.
17. Foster, R., Hu, K. Q., Lu, Y., Nolan, K. M., Thissen, J. & Settleman, J. (1996) *Mol. Cell Biol.* **16**, 2689–2699.
18. Clark, G. J., Kinch, M. S., Rogers-Graham, K., Sebti, S. M., Hamilton, A. D. & Der, C. J. (1997) *J. Biol. Chem.* **272**, 10608–10615.
19. Laxminarayan, K. M., Chan, B. K., Tetaz, T., Bird, P. I. & Mitchell, C. A. (1994) *J. Biol. Chem.* **269**, 17305–17310.
20. De Smedt, F., Boom, A., Pesesse, X., Schiffmann, S. N. & Erneux, C. (1996) *J. Biol. Chem.* **271**, 10419–10424.
21. De Angelis, D. A. & Braun, P. E. (1996) *J. Neurochem.* **66**, 2523–2531.
22. Braun, P. E., De Angelis, D., Shtybel, W. W. & Bernier, L. (1991) *J. Neurosci. Res.* **30**, 540–544.
23. Prendergast, G. C., Davide, J. P., deSolms, S. J., Giuliani, E. A., Graham, S. L., Gibbs, J. B., Oliff, A. & Kohl, N. E. (1994) *Mol. Cell. Biol.* **14**, 4193–4202.
24. Bishop, W. R., Bond, R., Petrin, J., Wang, L., Patton, R., Doll, R., Njoroge, G., Catino, J., Schwartz, J., Windsor, W., *et al.* (1995) *J. Biol. Chem.* **270**, 30611–30618.
25. Barrington, R. E., Subler, M. A., Rands, E., Omer, C. A., Miller, P. J., Hundley, J. E., Koester, S. K., Troyer, D. A., Bearss, D. J., Conner, M. W., *et al.* (1998) *Mol. Cell Biol.* **18**, 85–92.
26. Vogt, A., Sun, J., Qian, Y., Hamilton, A. D. & Sebti, S. M. (1997) *J. Biol. Chem.* **272**, 27224–27229.
27. Lebowitz, P. F., Sakamuro, D. & Prendergast, G. C. (1997) *Cancer Res.* **57**, 708–713.
28. Aaronson, S. A. & Weaver, C. A. (1971) *J. Gen. Virol.* **13**, 245–252.
29. Herzog, C. R., Soloff, E. V., McDoniels, A. L., Tyson, F. L., Malkinson, A. M., Haugen-Strano, A., Wiseman, R. W., Anderson, M. W. & You, M. (1996) *Oncogene* **13**, 1885–1891.
30. Krishan, A. (1975) *J. Cell Biol.* **66**, 188–193.
31. Schmid, I., Uittenbogaart, C. H. & Giorgi, J. V. (1994) *Cytometry* **15**, 12–20.
32. Gimona, M., Kazzaz, J. A. & Helfman, D. M. (1996) *Proc. Natl. Acad. Sci. USA* **93**, 9618–9623.
33. Prakash, V. & Timasheff, S. N. (1982) *J. Biol. Chem.* **258**, 1689–1697.
34. Moasser, M. M., Sepp-Lorenzino, L., Kohl, N. E., Oliff, A., Balog, A., Su, D. S., Danishefsky, S. J. & Rosen, N. (1998) *Proc. Natl. Acad. Sci. USA* **95**, 1369–1374.
35. Laezza, C., Wolff, J. & Bifulco, M. (1997) *FEBS Lett.* **413**, 260–264.
36. De Angelis, D. A. & Braun, P. E. (1994) *J. Neurosci. Res.* **39**, 386–397.
37. Cowley, S., Paterson, H., Kemp, P. & Marshall, C. J. (1994) *Cell* **77**, 841–852.
38. Mansour, S. J., Matten, W. T., Hermann, A. S., Candia, J. M., Rong, S., Fukasawa, K., Van de Woude, G. F. & Ahn, N. G. (1994) *Science* **265**, 966–970.
39. Reszka, A. A., Bulinski, J. C., Krebs, E. G. & Fischer, E. H. (1997) *Mol. Biol. Cell* **8**, 1219–1232.
40. Reszka, A. A., Seger, R., Diltz, C. D., Krebs, E. G. & Fischer, E. H. (1995) *Proc. Natl. Acad. Sci. USA* **92**, 8881–8885.